A distributed control strategy for optimal reactive power flow with power and voltage constraints

Saverio Bolognani
MIT
Cambridge (MA), USA
Email: saverio@mit.edu

Ruggero Carli
University of Padova
Padova, Italy
Email: carlirug@dei.unipd.it

Guido Cavraro
University of Padova
Padova, Italy
Email: cavraro@dei.unipd.it

Sandro Zampieri
University of Padova
Padova, Italy
Email: zampi@dei.unipd.it

***Abstract*—We consider the problem of exploiting the microgenerators connected to the power distribution network to provide distributed reactive power compensation for power losses minimization and voltage support. The proposed strategy relies on the fact that all the intelligent agents, located at the microgenerator buses, can measure their voltage, communicate data with other agents on a cyber-layer, and adjust the amount of reactive power injected into the grid according to a feedback control law that descends from duality-based methods applied to the optimal reactive power flow problem. We provide numerical simulations to verify the effectiveness of the proposed algorithm and we discuss its innovative feedback nature.**

I. Introduction

Recent technological advances, together with environmental and economic challenges, have been motivating the deployment of small power generators in the low voltage and medium voltage power distribution grid. The availability of a large number of these generators in the distribution grid can yield relevant benefits to the network operation. Indeed, they can be used to provide a number of ancillary services that are of great interest for the management of the grid [1], [2]. In particular, many inverters have the capability, when they are running below their rated output current, to inject (or to absorb) reactive power together with active power [3]. With respect to the traditional devices, such as shunt capacitor banks or on-load tap changers [4], the inverters can act in the grid on a fast timescale. In this paper we focus on the *optimal reactive power flow* (ORPF) problem. This problem has been deeply studied for the traditional transmission grid and is tipically solved by solvers that collect all the necessary field data, compute the optimal configuration, and dispatch the reactive power production to the generators, in a centralized manner. However this approach is not practical in the distribution network, because there is faster variability in the power demand, the availability of small size generators is hard to predict, and because generators can connect or disconnect, requiring an automatic reconfiguration of the grid control infrastructure (the so called " plug and play "approach). These reasons suggest a distributed approach to this problem. One of the most popular solution is to reformulate the ORPF problem as a rank-constrained semidefinite program, to convexify it by dropping the rank constraint and then to solve it in a distributed way (see for example [5], [6], [7]). This approach however requires that all the buses of the grid are monitored, which may not be practical. Instead, the algorithm proposed in [8], [9] are truly scalable in the number of generators and do not require monitoring of all the buses of the grid. These algorithms consist of the iteration of the two following actions: collecting voltage measurements at the microgenerators buses and actuating control laws based on these measured data. We refer to this kind of algorithms as *feedback control strategies*. Both the algorithm in [8] and the algorithm in [9] are shown to be provably convergent to the optimal solution of a convexified version of the ORPF problem and, also numerically, they exhibited promising performance. However in [8] no constraints either on the magnitude of voltages or on the amount of power injected by the microgenerators are considered, while in [9] only constraints on the voltages are included. In the same spirit of [9], in this paper we propose a feedback control strategy which is based on a dual ascent algorithm applied to the power distribution losses functional cost, incorporating both reactive power generation constraints and voltage magnitude limits.

The rest of the paper is organized as follows. In Section III, we provide a model for the cyber-physical system of a smart power distribution grid. In Section IV, we state the ORPF problem with power and voltage magnitude constraints. In Section V we first convexify the ORPF problem, adopting a suitable linearization of the power flow equation, and we derive the feedback control algorithm. In Section VI we provide both a synchronous and an asynchronous version of the algorithm. Finally in Section VII we provide some numerical results.

II. Mathematical Preliminaries and Notation

Let $\mathcal{G} = (\mathcal{V}, \mathcal{E}, \sigma, \tau)$ be a directed graph, where $\mathcal{V}$ is the set of nodes, $\mathcal{E}$ is the set of edges, with $n = |\mathcal{V}|, r = |\mathcal{E}|$. Moreover $\sigma, \tau : \mathcal{E} \to \mathcal{V}$ are two functions such that edge $e \in \mathcal{E}$ goes from the source node $\sigma(e)$ to the terminal node $\tau(e)$. Given two nodes of the graph $h, k \in \mathcal{V}$, we define the path $\mathcal{P}_{hk} = (v_1, \dots, v_\ell)$ as the sequence of nodes, without repetitions, such that $v_1 = h$, $v_\ell = k$ and for each $i = 1, \dots, \ell - 1$, the nodes v_i and v_{i+1} are connected by an edge (regardless of its direction). In the rest of the paper we will often introduce complex-valued functions defined on the nodes and on the edges. These functions will also be intended as vectors in $\mathbb{C}^n$ and $\mathbb{C}^r$. Given a vector u, we denote by $\bar{u}$ its (element-wise) complex conjugate, and by u^T its transpose. We denote by $\Re(u)$ and by $\Im(u)$ the real and the imaginary part of u, respectively. Let $A \in \{0, \pm 1\}^{r \times n}$ be the incidence

The research leading to these results has received funding from the European Communitys Seventh Framework Program under grant agreement n. 257462 HYCON2 Network of Excellence.

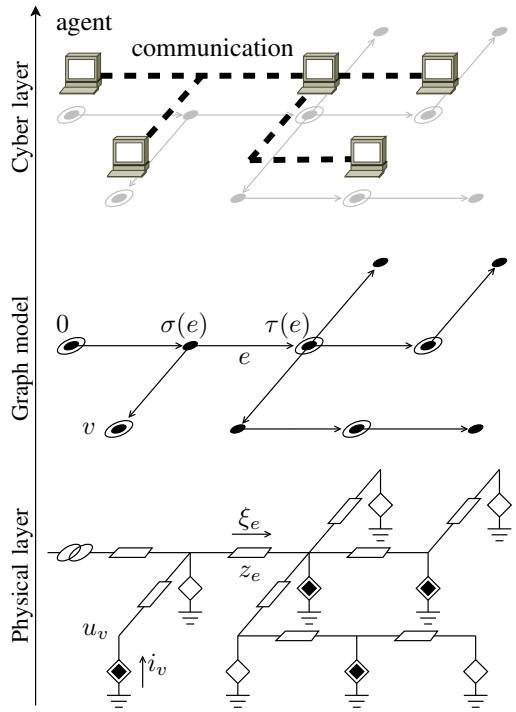

Figure 1. Schematic representation of a microgrid. In the lower panel the physical layer is represented via a circuit representation, where black diamonds are microgenerators, white diamonds are loads, and the left-most element of the circuit represents the PCC. The middle panel illustrates the corresponding graph representation. The upper panel represents the cyber layer, where agents (i.e. microgenerators and the PCC) are connected via a communication infrastructure.

matrix of the graph $\mathcal{G}$, defined via its elements

$$[A]_{ev} = \begin{cases} -1 & \text{if } v = \sigma(e) \\ 1 & \text{if } v = \tau(e) \\ 0 & \text{otherwise.} \end{cases}$$

We define by $\mathbf{1}$ the column vector of all ones, while by $\mathbf{1}_v$ we denote the vector whose value is 1 in position v, and 0 everywhere else. Given $u, v, w \in \mathbb{R}^\ell$, with $v_h \leq w_h, h = 1, \ldots, \ell$ we define the operator $\text{proj}(u, v, w)$ as the component wise projection of u in the set $\left\{x \in \mathbb{R}^\ell : v_h \leq x_h \leq w_h, h = 1, \ldots, \ell\right\}$, that is,

$$[\text{proj } (u, v, w)]_h = \begin{cases} u_h & \text{if } v_h \leq u_h \leq w_h \\ v_h & \text{if } u_h < v_h \\ w_h & \text{if } u_h > w_h \end{cases} \quad (1)$$

III. Cyber-physical model of a smart power distribution grid

In this work, we envision a *smart* power distribution network as a cyber-physical system, in which the *physical layer* consists of the power distribution infrastructure, including power lines, loads, microgenerators, and the point of connection to the transmission grid, while the *cyber layer* consists of intelligent agents, dispersed in the grid, and provided with actuation, sensing, communication, and computational capabilities. We model the physical layer as a directed graph $\mathcal{G}$, in which edges in $\mathcal{E}$ represent the power lines, and nodes in $\mathcal{V}$ represent both loads and generators that are connected to the microgrid (see Figure 1, middle panel). These include the residential and industrial consumers, microgenerators, and also the point of connection of the microgrid to the transmission grid (called point of common coupling, or PCC). We limit our study to the steady state behavior of the system, where all voltages and currents are sinusoidal signals at the same pulsation ω_0, and are therefore represented by complex quantities.

The system state is described by the following system variables (see Figure 1, lower panel):

- $u \in \mathbb{C}^n$, where u_v is the grid voltage at node v;
- $i \in \mathbb{C}^n$, where i_v is the current injected at node v;
- $\xi \in \mathbb{C}^r$, where ξ_e is the current flowing on edge e.
- $s = p + iq \in \mathbb{C}^r$, where s_v, p_v and q_v are the complex, the active and the reactive power injected at node v.

For every edge e of the graph, we define by z_e the impedance of the corresponding power line. We assume the following.

Assumption 1: All power lines in the grid have the same inductance/resistance ratio, i.e., $z_e = e^{j\theta}|z_e|$, for any e in $\mathcal{E}$ and for a fixed θ.

Assumption 1 is satisfied when the grid is relatively homogeneous, and is reasonable in most practical cases. The following equations (Kirchhoff's current and voltage law) are satisfied by u, i and ξ:

$$A^T \xi + i = 0, \quad (2)$$

$$Au + e^{j\theta} Z \xi = 0, \quad (3)$$

where Z denotes the diagonal matrix of the absolute values of the line impedances, namely, Z=diag$(|z_e|, e \in \mathcal{E})$.

We label the PCC as node 0 and take it as an ideal sinusoidal voltage generator (*slack bus*) at the microgrid nominal voltage U_N, with arbitrary, but fixed, angle ϕ

$$u_0 = U_N e^{i\phi} . \quad (4)$$

Each node v of the grid (load or microgenerator) except the PCC is characterized via the following law relating its injected current i_v with its voltage u_v

$$u_v \bar{i}_v = s_v, \quad \forall v \in \mathcal{V} \backslash \{0\}, \quad (5)$$

i.e., all nodes but the PCC are being modeled as *constant power* or *P-Q buses*. The powers s_v corresponding to grid loads are such that $p_v < 0$, meaning that positive active power is *supplied* to the devices. The complex powers corresponding to microgenerators, on the other hand, are such that $p_v \geq 0$, as positive active power is *injected* into the grid [10].

We assume that every microgenerator, and also the PCC, corresponds to an *agent* in the cyber layer (see the upper panel of Figure 1). We denote this subset of the nodes of $\mathcal{G}$ by $\mathcal{C}$ (with $|\mathcal{C}| = m$). Each agent is provided with sensing capability in the form of a phasor measurement unit (PMU, i.e., a sensor measuring voltage amplitude and angle [11]). Agents that correspond to microgenerators can command the amount of reactive power injected in the grid. Moreover agents can communicate with each other, via some communication channels which could possibly via power line communication (PLC). Motivated by this possibility, we define the neighbors in the cyber layer in the following way.

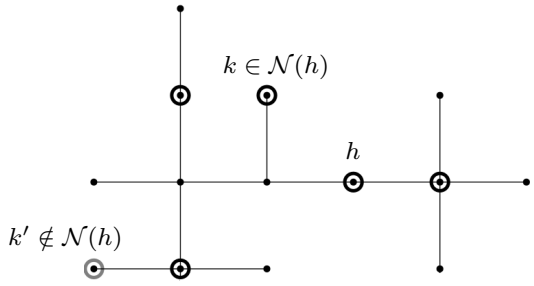

Figure 2. An example of neighbor agents in the cyber layer. Circled nodes (both gray and black) are agents (nodes in $\mathcal{C}$). Nodes circled in black belong to the set $\mathcal{N}(h) \subset \mathcal{C}$. Node circled in gray are agents which do not belong to the set of neighbors of h. For each agent $k \in \mathcal{N}(h)$, the path that connects h to k does not include any other agent besides h and k themselves.

Definition 2 (Neighbors in the cyber layer): Let $h \in \mathcal{C}$ be an agent of the cyber layer. The set of neighbors of h in the cyber layer, denoted as $\mathcal{N}(h)$, is the subset of $\mathcal{C}$ defined as

$$\mathcal{N}(h) = \{k \in \mathcal{C} \mid \forall \mathcal{P}_{hk}, \mathcal{P}_{hk} \cap \mathcal{C} = \{h, k\}\}.$$

Figure 2 gives an example of such set. In the rest of the paper we assume that every agent $h \in \mathcal{C}$ knows its set of neighbors $\mathcal{N}(h)$, and can communicate with them.
We conclude the section by introducing the following block decomposition for the vectors of voltages u and powers s

$$u = [u_0 \quad u_G \quad u_L]^T, \quad s = [s_0 \quad s_G \quad s_L]^T, \tag{6}$$

where u_0 is the voltage at the PCC, $u_G \in \mathbb{C}^{m-1}$ and $u_L \in \mathbb{C}^{n-m}$ are the voltages at the microgenerators and at the loads respectively. Similarly for $s_G = p_G + jq_G$ and $s_L = p_L + jq_L$.

IV. Optimal reactive power flow problem

We consider the problem of commanding the reactive power injection at the microgenerators to minimize power distribution losses, while satisfying some operational constraints. Specifically, we want to guarantee that the voltages magnitudes stay in a opportune neighbourhood of the nominal voltage, and to take into account the reactive power generation capability of each microgenerator. The decision variables are the reactive power commands $q_h, h \in \mathcal{C}\backslash\{0\}$. Power distribution losses can be expressed, by using (3), as

$$J_{\text{losses}} := \sum_{e \in \mathcal{E}} |\xi_e|^2 \Re(z_e) = \bar{u}^T L u. \tag{7}$$

Given a upper bound $q^{\max} \in \mathbb{C}^{m-1}$ (resp. a lower bound $q^{\min}$), where $q_v^{\max}$ (resp. $q_v^{\min}$) represents the maximum (resp. minimum) amount of reactive power that the v-th compensator can inject into the grid, and given a upper bound $U_{\max}$ (resp. a lower bound $U_{\min}$) for the voltage magnitudes, we can formulate the following optimization problem,

$$\min_{q_h, h \in \mathcal{C}\backslash\{0\}} \quad \bar{u}^T L u \tag{8a}$$

$$\text{subject to} \quad q_h^{\min} \le q_h \le q_h^{\max}, \quad \forall h \in \mathcal{C}\backslash\{0\} \tag{8b}$$

$$U_{\min}^2 \le |u_h|^2 \le U_{\max}^2, \quad \forall h \in \mathcal{C}\backslash\{0\} \tag{8c}$$

Assumption 3: There exists a minimizer of (8a) that satisfies the constraints (8b) and (8b).

While (8b) represents the typical constraints in the reactive power generation capabilities, (8c) is a bit different from the classical ORPF voltages constraints formulation, which, in general, imposes constraints on the voltages of all the nodes. This difference is due to the fact that, in our setup, only the generators are provided with sensing capabilities and, in turn, only their voltages can be measured and controlled.
From a system-wide prospective, the control problem that we are considering is characterized by, the input variables q_G, the measured output variables u_0, u_G and the unmeasured disturbances p_L, q_L, p_G. It is worth remarking the decision variables of the ORPF problem (i.e., the input variables q_G) do not include the reactive power provided by the PCC (i.e., $q_0 = u_0 \bar{i}_0$). However also this quantity will change when the reactive power injections of the generators are modified by the algorithm, because of the inherent physical behavior of the slack bus (the PCC).

V. A dual-ascent like algorithm

Problem (8) is not convex in general, due to the non-linear relations between the voltages and the powers injected by the node. In this section, we introduce an approximated solution of the nonlinear equations (2), (3), (4), and (5), to covexify the ORPF problem (8) and to derive a *dual ascent algorithm* [12] to be implemented by the microgenerators. To do so, we first need the following technical lemma (see [9]).

Lemma 4: Let L be the bus admittance matrix of the grid. Then, there exists a unique symmetric, positive semidefinite matrix $X \in \mathbb{R}^{n \times n}$ such that

$$\begin{cases} XL = I - \mathbf{1}\mathbf{1}_0^T \\ X\mathbf{1}_0 = 0. \end{cases} \tag{9}$$

The matrix X depends only on the topology of the grid power lines and on their impedances. By adopting the same block decomposition as in (6), we have

$$X = \begin{bmatrix} 0 & 0 & 0 \\ 0 & M & N \\ 0 & N^T & O \end{bmatrix}, \tag{10}$$

with $M \in \mathbb{R}^{(m-1)\times(m-1)}$, $N \in \mathbb{R}^{(m-1)\times(m-n)}$, and $O \in \mathbb{R}^{(n-m)\times(n-m)}$. The following proposition (see [9]) provides the approximate relation between the grid voltages and the power injections at the nodes.

Proposition 5: Consider the physical model described by the set of nonlinear equations (2), (3), (4), and (5). Node voltages then satisfy

$$\begin{bmatrix} u_0 \\ u_G \\ u_L \end{bmatrix} = e^{j\phi} \left(U_N \mathbf{1} + \frac{e^{j\theta}}{U_N} \begin{bmatrix} 0 & 0 & 0 \\ 0 & M & N \\ 0 & N^T & O \end{bmatrix} \begin{bmatrix} 0 \\ \bar{s}_G \\ \bar{s}_L \end{bmatrix} \right) + o\left(\frac{1}{U_N}\right),$$

where the little-o notation means that $\lim_{U_N \to \infty} \frac{o(f(U_N))}{f(U_N)} = 0$.

The quality of this approximation relies on having large nominal voltage U_N and relatively small currents injected by the inverters (or supplied to the loads). This assumption

is verified in practice, and corresponds to correct design and operation of power distribution networks. In some sense this approximation extends the DC power flow model to the lossy case. Given the the voltages u expression presented in Proposition 5, we can write after some algebraic computations

$$\bar{u}^T L u = \frac{p^T X p}{U_N^2} + \frac{q^T X q}{U_N^2} + o\left(\frac{1}{U_N^2}\right) \tag{11a}$$

$$|u_G|^2 = 2\,[M \quad N]\,[\cos(\theta)p + \sin(\theta)q] + \mathbf{1}U_N^2 + o(1), \tag{11b}$$

where, with a slight abuse of notation, by $|u_G|^2$ we denote the vector collecting all the squared voltage magnitudes at the microgenerators. By neglecting in (11b) the $o(1)$ terms (that goes to zero as U_N tends to infinity), the non-linear constraint (8c) (w.r.t. the control variable q_G) reduces to the following two linear inequalities

$$\mathbf{1}U_{\min}^2 \leq 2\,[M \quad N] \begin{bmatrix} \cos(\theta)p_G + \sin(\theta)q_G \\ \cos(\theta)p_L + \sin(\theta)q_L \end{bmatrix} + \mathbf{1}U_N^2 \leq \mathbf{1}U_{\max}^2.$$

Furthermore, expression in (11a) without the $o(1/U_N^2)$ term, can be used to convexify (8), leading to the following convex OPRF problem

$$\min_{q_h, h\in\mathcal{C}\backslash\{0\}} \quad q_G^T \frac{M}{2} q_G + q_G^T N q_L \tag{12a}$$

$$\text{subject to} \quad q_h^{\min} \leq q_h \leq q_h^{\max}, \quad \forall h \in \mathcal{C}\backslash\{0\} \tag{12b}$$

$$U_{\min}^2 \leq |u_h|^2 \leq U_{\max}^2, \quad \forall h \in \mathcal{C}\backslash\{0\} \tag{12c}$$

The Lagragian associated to (12) is

$$\begin{aligned}\mathcal{L}(q_G, \underline{\mu}, \overline{\lambda}, \underline{\mu}, \overline{\mu}) = q_G^T \frac{M}{2} q_G + q_G^T N q_L + \\ + \underline{\lambda}^T \left(\mathbf{1}U_{\min}^2 - |u_G|^2\right) + \overline{\lambda}^T \left(|u_G|^2 - \mathbf{1}U_{\max}^2\right) + \\ + \underline{\mu}^T \left(q^{\min} - q_G\right) + \overline{\mu}^T \left(q_G - q^{\max}\right)\end{aligned} \tag{13}$$

The idea, to solve the above problem, is to resort to a dual ascent algorithm which iteratively cycles the dual ascent steps on the multipliers $\underline{\lambda}, \overline{\lambda}, \underline{\mu}, \overline{\mu}$ and the minimization step of $\mathcal{L}$ w.t.r. to the primal variable q_G. It is well know, however, that this procedure guarantees the primal feasibility of the asymptotic solution, but not the primal feasibility of each intermediate step. This might be acceptable for the voltage constraints (12c), in the meaning that voltage constraints can be intended as *soft constraints*, since they do not derive from physical constraints on the system, and their violation can be tolerated if it affects the system for a small time lapse. On the contrary, constraints (12b) have to be guaranteed at each iteration, since they stems from physical limitations of the generators, and they have to be intended as *hard constraints*. Based on the above observation, we next propose a dual-ascent like algorithm which guarantees the *hard constraints* to be satisfied at each iteration. This algorithm consists in the iterative execution of the following alternated steps:

1) update of the multipliers

$$\underline{\lambda}(t+1) = \left[\underline{\lambda}(t) + \gamma_{\underline{\lambda}} \frac{\partial \mathcal{L}(q_G(t), \underline{\lambda}(t), \overline{\lambda}(t), \underline{\mu}(t), \overline{\mu}(t))}{\partial \underline{\lambda}}\right]_+,$$

$$\overline{\lambda}(t+1) = \left[\overline{\lambda}(t) + \gamma_{\overline{\lambda}} \frac{\partial \mathcal{L}(q_G(t), \underline{\lambda}(t), \overline{\lambda}(t), \underline{\mu}(t), \overline{\mu}(t))}{\partial \overline{\lambda}}\right]_+,$$

2) computation of the minimum w.r.t. the primal variable q_G

$$\bar{q}_G = \arg\min_{q_G} \mathcal{L}(q_G, \underline{\lambda}(t+1), \overline{\lambda}(t+1), \underline{\mu}(t), \overline{\mu}(t)),$$

3) update of the multipliers

$$\underline{\mu}(t+1) = \left[\underline{\mu}(t) + \gamma_{\underline{\mu}} \frac{\partial L(\bar{q}_G, \underline{\lambda}(t+1), \overline{\lambda}(t+1), \underline{\mu}(t), \overline{\mu}(t))}{\partial \underline{\mu}}\right]_+, \tag{15a}$$

$$\overline{\mu}(t+1) = \left[\overline{\mu}(t) + \gamma_{\overline{\mu}} \frac{\partial \mathcal{L}(\bar{q}_G, \underline{\lambda}(t+1), \overline{\lambda}(t+1), \underline{\mu}(t), \overline{\mu}(t))}{\partial \overline{\mu}}\right]_+, \tag{15b}$$

4) actuation of $\bar{q}_G$ projected in the feasible set

$$q_G(t+1) = \text{proj}\,(\bar{q}_G, q^{\max})$$

In the above expressions the $[\cdot]_+$ operator corresponds to the projection on the positive orthant; moreover $\gamma_{\underline{\lambda}}$, $\gamma_{\overline{\lambda}}$, $\gamma_{\underline{\mu}}$ and $\gamma_{\overline{\mu}}$ are suitable positive constants *a-priori* assigned. By simple computations, it turns out from (13) that the update of the multipliers can be rewritten as

$$\underline{\lambda}(t+1) = \left[\underline{\lambda}(t) + \gamma_{\underline{\lambda}} \left(\mathbf{1}U_{\min}^2 - |u_G|^2\right)\right]_+ \tag{16a}$$

$$\underline{\lambda}(t+1) = \left[\overline{\lambda}(t) + \gamma_{\overline{\lambda}} \left(|u_G|^2 - \mathbf{1}U_{\max}^2\right)\right]_+ \tag{16b}$$

$$\underline{\mu}(t+1) = \left[\underline{\mu}(t) + \gamma_{\underline{\mu}} \left(q^{\min} - \bar{q}_G\right)\right]_+, \tag{16c}$$

$$\overline{\mu}(t+1) = \left[\overline{\mu}(t) + \gamma_{\overline{\mu}} \left(\bar{q}_G - q^{\max}\right)\right]_+, \tag{16d}$$

and that the minimization, w.r.t. the primal variable q_G, is achieved by letting

$$\begin{aligned}\bar{q}_G = &- M^{-1} N q_L + 2\sin(\theta)(\underline{\lambda}(t+1) - \overline{\lambda}(t+1)) \\ &+ M^{-1}(\underline{\mu}(t) - \overline{\mu}(t))\end{aligned} \tag{17}$$

VI. Synchronous and asynchronous algorithm

In this section, we show how the algorithm proposed in the previous section can be implemented by the agents in $\mathcal{C}\backslash\{0\}$. To do so, we first introduce the following matrix G.

Lemma 6: There exists a unique symmetric matrix $G \in \mathbb{R}^{m\times m}$, such that

$$\begin{cases} \begin{bmatrix} 0 & 0 \\ 0 & M \end{bmatrix} G = I - \mathbf{1}\mathbf{1}_0^T \\ G\mathbf{1} = 0. \end{cases}$$

It could be easily proved that G is the Kron reduction of $\boldsymbol{X}$ with respect to the compensators components.

Lemma 7: The matrix G has the sparsity pattern induced by the Definition 2 of neighbor agents in the cyber layer, i.e.

$$G_{hk} \neq 0 \quad \Leftrightarrow \quad k \in \mathcal{N}(h).$$

Next we propose the following algorithm, assuming that the agents are coordinated, i.e., they can update their state variables q_h and λ_h, $h \in \mathcal{C}\backslash\{0\}$, synchronously.

Let all agents store the auxiliary scalar variables $\underline{\lambda}_h$, $\overline{\lambda}_h$, $\underline{\mu}_h$ and $\overline{\mu}_h$. Let $\gamma_{\underline{\lambda}}$, $\gamma_{\overline{\lambda}}$, $\gamma_{\underline{\mu}}$ and $\gamma_{\overline{\mu}}$ be positive scalar parameters, and let θ be the impedance angle defined in Assumption 1. Let G_{hk} be the elements of the matrix G defined in Lemma 6. At every synchronous iteration of the algorithm, each agent $h \in \mathcal{C}\backslash\{0\}$ executes the following operations in order:

1) gathers the voltage measurements
$$\{u_k = |u_k|e^{j\angle u_k}, k \in \mathcal{N}(h)\}$$
and the multipliers $\underline{\mu}_k$ and $\overline{\mu}_k$ from its neighbors;
2) updates the auxiliary variables $\underline{\lambda}_h$ and $\overline{\lambda}_h$ as
$$\underline{\lambda}_h \leftarrow \left[\underline{\lambda}_h + \gamma_{\underline{\lambda}_h}\left(\mathbf{1}U_{\min}^2 - |u_G|^2\right)\right]_+ \quad (18a)$$
$$\overline{\lambda}_h \leftarrow \left[\overline{\lambda}_h + \gamma_{\overline{\lambda}}\left(|u_G|^2 - \mathbf{1}U_{\max}^2\right)\right]_+ \quad (18b)$$
3) computes the optimal reactive power q_h regardless of the generation capability as
$$q_h \leftarrow \sum_{k\in\mathcal{N}(h)\cup h} G_{hk}(|u_h||u_k|\sin(\angle u_k - \angle u_h - \theta) + \\ + (\underline{\mu}_k - \overline{\mu}_k)) + q_h + 2\sin(\theta)(\underline{\lambda}_h - \overline{\lambda}_h) \quad (19)$$
4) updates the auxiliary variables $\underline{\mu}_h$ and $\overline{\mu}_h$ as
$$\underline{\mu}_h \leftarrow \left[\underline{\mu}_h + \gamma_{\underline{\mu}_h}\left(q_h^{\min} - q_h\right)\right]_+ \quad (20a)$$
$$\overline{\mu}_h \leftarrow \left[\overline{\mu}_h + \gamma_{\overline{\mu}}\left(q_h - q_h^{\max}\right)\right]_+ \quad (20b)$$
5) projects q_h into the feasible region, i.e.,
$$q_h \leftarrow \text{proj}\ \left(q_h, q_h^{\min}, q_h^{\max}\right) \quad (21)$$
and actuates this projected value of q_h.

It can be shown, by using Lemma 7 and via some algebraic manipulations, that the update (19) can be rewritten as
$$q_G \leftarrow M^{-1}(\underline{\mu}(t) - \overline{\mu}(t)) + 2\sin(\theta)(\underline{\lambda}(t+1) - \overline{\lambda}(t+1)) + \\ + q_G(t) + \Im\left(e^{-j\theta}\begin{bmatrix}0 & \text{diag}(\bar{u}_G)\end{bmatrix} G \begin{bmatrix}u_0 \\ u_G\end{bmatrix}\right),$$
which, by using the expression for u provided by Proposition 5, is equal to
$$q_G \leftarrow -M^{-1}Nq_L + 2\sin(\theta)(\underline{\lambda} - \overline{\lambda}) \\ + M^{-1}(\underline{\mu} - \overline{\mu}) + o\left(\frac{1}{U_N}\right).$$
Comparing this expression for q_G with the expression in (17), it turns out that q_G minimizes the Lagrangian with respect to the primal variables, up to a term that vanishes for large U_N.

In order to avoid the burden of coordination among the agents, we also propose an asynchronous version of the algorithm, in which the agents update their state $(q_h, \underline{\lambda}_h, \overline{\lambda}_h, \underline{\mu}_h, \overline{\mu}_h)$ independently one from the other. We assume that each agent is provided with an individual timer, by which it is triggered. Timers tick randomly, with exponentially, identically distributed waiting times. When an agent is triggered, it gathers the voltage measurements and the multipliers from its neighbors, and then executes the operations explained in (18), (19), (20) and (21), while variables of all the other agents are kept fixed.

Remark 8: Notice that the proposed algorithm requires the interleaving of actuation and sensing, and therefore the control action is a function of the real time measurements. The compensators active power injections and the power injection of the loads can be considered as disturbances for the control system. As it happens in all feedback control systems, these quantities do not need to be known to the controller: in some sense, the agents are implicitly inferring this information from the voltage measurements. the proposed strategy exhibits this kind of robustness. This feature differentiates the proposed algorithm from most of the OPF algorithms available in the literature.

VII. Simulations

The algorithm has been tested on the testbed IEEE 37 [16]. The load buses are a blend of constant-power, constant-current, and constant-impedance loads, with a total power demand of almost 2 MW of active power and 1 MVAR of reactive power (see [16] for the testbed data). The impedance of the power lines differs from edge to edge, however, the inductance/resistance ratio exhibits a smaller variation, ranging from $\angle z_e = 0.47$ to $\angle z_e = 0.59$ (justifying in some sense Assumption 1). We considered the scenario in which 6 microgenerators have been deployed in this portion of the power distribution grid (see Figure 3).

The deviation tolerated from nominal voltage magnitude for the micro-generators has been set to 3%. Both the synchronous and the asynchronous algorithms have been simulated on a nonlinear exact solver of the grid [17]. We have numerically set $\gamma_{\underline{\lambda}} = \gamma_{\overline{\lambda}} = 5.75$ and $\gamma_{\underline{\mu}} = \gamma_{\overline{\mu}} = 0.02$ (a suggestion on how to choose them is given in [9]). Timers in the asynchronous case have been tuned so that each agent is triggered, in expectation, at the same rate of the synchronous case. A time-varying profile for the loads has been generated, in order to simulate the effect of slowly varying loads (e.g. the aggregate demand of a residential neighborhood), fast changing demands (e.g. some industrial loads), and intermittent large loads (e.g. heating). The results of the simulation have been plotted in Figure 4. For both the synchronous and the asynchronous case, the power distribution losses, the lowest voltage magnitude measured by the microgenerators (but not the highest, because in a reducing losses scenario the upper bound had been never excited) and a significant reactive power injection trajectory are reported.It can be seen that the proposed algorithm achieves practically the same performance of the centralized solver, in terms of power distribution losses, without however having access to the unmonitored demands of the loads. Notice moreover that, since for duality based methods the voltage constraint is satisfied only at the steady state, in the time varying case simulated the voltage sometimes falls lightly below the prescribed threshold, when the power demand of the loads present abrupt changes. This could leave to the possibility that, only temporarily until the operative constraints are satisfied, the losses due to the algorithm are smaller than the optimal one. This effect is even more noticeable in

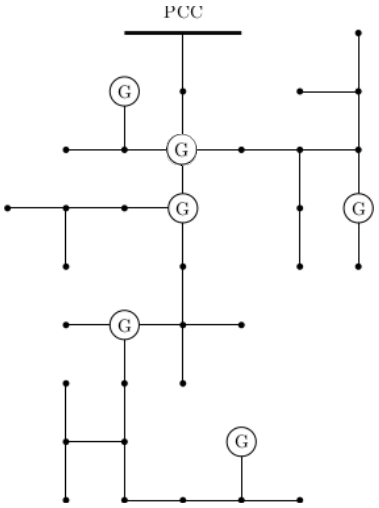

Figure 3. Schematic representation of the IEEE 37 test feeder [16], where 5 microgenerators have been deployed.

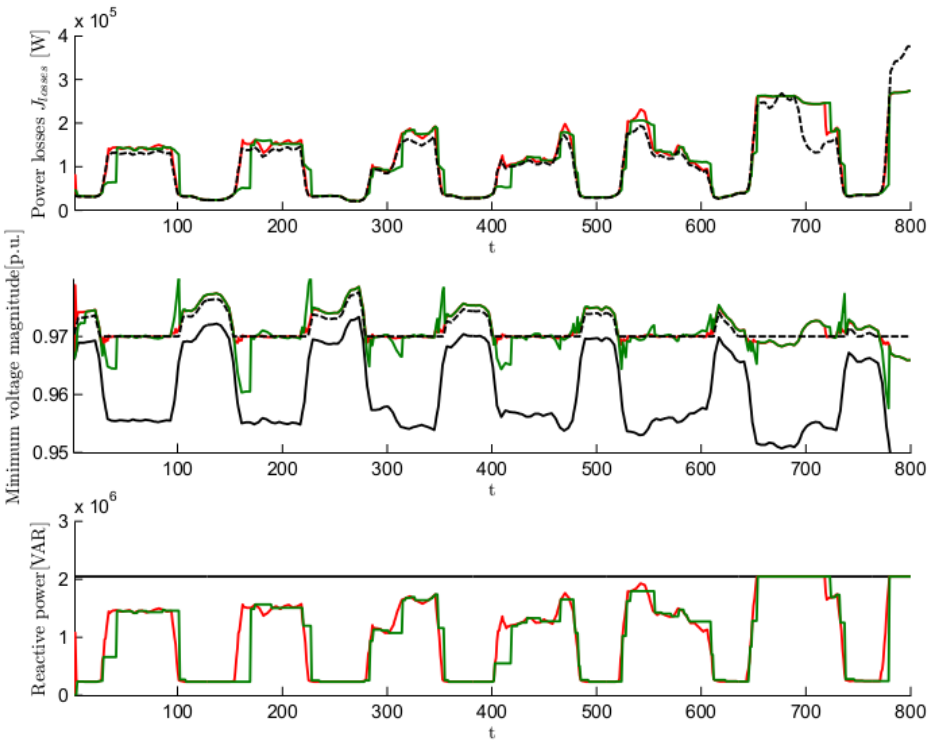

Figure 4. **Upper panel:** power losses achieved by a centralized controller (black dashed line) and by the proposed algorithm (synchronous/red and asynchronous/green). **Middle panel:** lowest bus voltage achieved by a centralized controller (black dashed line) and by the proposed algorithm (synchronous/red and asynchronous/green). The black solid line represents the case of no reactive power compensation. **Lower panel:** reactive power injection by one of the generators in the synchronous/red and in the asynchronous/green case, together with the corresponding constraint (black line).

the asynchronous case, where iteration times are not evenly spaced, but vanishes at steady state. It should be remarked, however, that the extent of this constraint violation depends on the rate at which the algorithms are executed, compared with the rate of variation of loads, and is ultimately a function of the communication resources available at the cyber level.

REFERENCES

[1] F. Katiraei and M. R. Iravani, "Power management strategies for a microgrid with multiple distributed generation units," *IEEE Trans. Power Syst.*, vol. 21, no. 4, pp. 1821–1831, Nov. 2006.

[2] M. Prodanovic, K. De Brabandere, J. Van den Keybus, T. Green, and J. Driesen, "Harmonic and reactive power compensation as ancillary services in inverter-based distributed generation," *IET Gener. Transm. Distrib.*, vol. 1, no. 3, pp. 432–438, 2007.

[3] K. Turitsyn, P. Šulc, S. Backhaus, and M. Chertkov, "Options for control of reactive power by distributed photovoltaic generators," *Proc. IEEE*, vol. 99, no. 6, pp. 1063–1073, Jun. 2011.

[4] M. E. Baran and F. F. Wu, "Optimal sizing of capacitors placed on a radial distribution system," *IEEE Trans. Power Del.*, vol. 4, no. 1, pp. 735–743, Jan. 1989.

[5] E. Dell'Anese, H. Zhu, and G. Giannakis, "Distributed optimal power flow for smart microgrids," *submitted to IEEE Transactions of Smart Grid*, 2013, arXiv preprint available [math.OC] 1211.5856.

[6] J. Lavaei and S. H. Low, "Zero duality gap in optimal power flow problem," *IEEE Trans. Power Syst.*, 2011.

[7] A. Lam, B. Zhang, A. Dominguez-Garcia, and D. Tse, "Optimal distributed voltage regulation in power distribution networks," *submitted to IEEE Transactions on Power System*, 2013, arXiv preprint available [math.OC] 1204.5226.

[8] A. Costabeber, T. Erseghe, P. Tenti, S. Tomasin, and P. Mattavelli, "Optimization of micro-grid operation by dynamic grid mapping and token ring control," in *Proc. 14th European Conf. on Power Electronics and Applications (EPE)*, Birmingham, UK, 2011.

[9] S. Bolognani, R. Carli, and S. Cavraro, G. Zampieri, "A distributed feedback control strategy for optimal reactive power flow with voltage constraints," 2012, arXiv preprint available 1303.7173.

[10] T. C. Green and M. Prodanović, "Control of inverter-based micro-grids," *Electr. Pow. Syst. Res.*, vol. 77, no. 9, pp. 1204–1213, Jul. 2007.

[11] A. G. Phadke, "Synchronized phasor measurements in power systems," *IEEE Comput. Appl. Power*, vol. 6, no. 2, pp. 10–15, Apr. 1993.

[12] D. P. Bertsekas, *Nonlinear programming*, 2nd ed. Belmont (MA): Athena Scientific, 1999.

[13] A. Ghosh, S. Boyd, and A. Saberi, "Minimizing effective resistance of a graph," *SIAM Rev.*, vol. 50, no. 1, pp. 37–66, Feb. 2008.

[14] A. Gómez-Expósito, A. J. Conejo, and C. Cañizares, *Electric energy systems. Analysis and operation*. CRC Press, 2009.

[15] S. Bolognani and S. Zampieri, "Convergence analysis of a distributed voltage support strategy for optimal reactive power compensation," in *Proc. NECSYS 2012, Santa Barbara (CA), USA*.

[16] W. H. Kersting, "Radial distribution test feeders," in *IEEE Power Engineering Society Winter Meeting*, vol. 2, Jan. 2001, pp. 908–912.

[17] R. D. Zimmerman, C. E. Murillo-Sánchez, and R. J. Thomas, "MATPOWER: steady-state operations, planning and analysis tools for power systems research and education," *IEEE Transactions on Power Systems*, vol. 26, no. 1, pp. 12–19, Feb. 2011.